

Quantum-dot helium: Effects of deviations from a parabolic confinement potential

Daniela Pfannkuche and Rolf R. Gerhardt

Max-Planck-Institut für Festkörperforschung, Heisenbergstrasse 1, D-7000 Stuttgart 80, Germany

(Received 15 August 1991)

The magneto-optical response to far-infrared radiation of quantum dots containing two electrons is studied theoretically. The symmetry-breaking effects of deviations from a strictly parabolic confinement potential are emphasized. We demonstrate the evidence of many-particle effects in systems where the generalized Kohn's theorem is no longer applicable. The calculated resonance spectrum reflects and explains all features observed in recent high-resolution measurements.

Quantum dots can be regarded as artificial atoms to which the electrons are bound by a "manufactured" confining potential. Usually arrays of such dots are prepared on semiconductor heterostructures, such that all of them contain the same number of electrons. Experimental conditions not only allow the number of electrons per dot to be tuned, thus switching from one quantum dot "element" to another,^{1,2} but also determine whether the individual atoms are isolated or couple with each other.³ Far infrared radiation (FIR) experiments provide some information about the internal level structure of the dots.¹⁻⁵

A convenient description for quantum dots assumes a parabolic confinement potential.⁶⁻⁹ In this exceptional case⁸ the electronic motion can be separated into an uncoupled center-of-mass (c.m.) motion and relative motion (RM). The Coulomb interaction, which only affects the RM, leads to a highly complicated energy spectrum and tends to shift the angular momentum of the RM ground state with increasing magnetic field to increasingly higher (absolute) values.^{6,7} The ground state of the two-electron system is given by the product of the c.m. and RM ground state. Since the angular momentum of the c.m. ground state remains zero, the total angular momentum of the quantum-dot helium ground state increases with increasing magnetic field according to the angular momentum of the RM. However, since the FIR only couples to the center-of-mass motion (the incident electric field is constant in a single dot), neither the features of the energy spectrum, which are specific for each quantum-dot element, nor the change in the angular momentum of the ground state can be detected for dots with purely parabolic confinement. According to the generalized Kohn's theorem^{6,9,10} the dipole-resonance frequencies are given by the one-particle excitation energies^{8,11,12}

$$\omega_{\pm} = \omega_{\text{eff}} \pm \frac{\omega_c}{2}, \quad (1)$$

where the effective frequency ω_{eff} is composed of the cyclotron frequency $\omega_c = eB/(m^*c)$ and the characteristic frequency of the confinement potential ω_0 ,

$$\omega_{\text{eff}} = \sqrt{\omega_c^2/4 + \omega_0^2}. \quad (2)$$

Here $m^* = 0.067m_0$ is the effective mass of an electron in GaAs.

The situation changes, if deviations from the parabolic confinement are taken into account^{11,13,14} or the response to electric fields with higher angular momenta is regarded.¹⁴ Under such conditions, as well as in the presence of a strong electrostatic coupling between neighboring dots,^{3,15} additional resonance frequencies occur. However, for most experiments^{2,4,5} the electrostatic coupling is of minor importance due to the large distance between neighboring dots.⁸

In this paper we consider the magneto-optical response to FIR of quantum-dot helium, accounting for deviations from the parabolic confinement. In contrast to recent work by Gudmundsson and Gerhardt,¹⁴ who used a self-consistent Hartree-random-phase-approximation (RPA) method, we calculate the two-particle energy spectrum by exact diagonalization of the Hamiltonian. This approach allows for a detailed study of the symmetry-breaking mechanisms leading to the experimentally observed splitting of the ω_+ mode^{2,5} and the mode coupling reflected in an anti-crossing behavior of this mode at smaller magnetic fields.⁵

We use the basis function set of the noninteracting two-electron system in a circular-symmetric parabolic confinement potential. This is the product basis of the c.m. and RM wave functions,

$$|n_C M_C n_R M_R\rangle = |n_C M_C\rangle |n_R M_R\rangle, \quad (3)$$

with C and R denoting the c.m. and the RM coordinates, respectively. Both the c.m. Hamiltonian and the RM Hamiltonian yield the same energy spectrum

$$\varepsilon_{nM} = (2n + |M| + 1)\hbar\omega_{\text{eff}} + M\frac{\hbar}{2}\omega_c, \quad (4)$$

which equals the one-electron spectrum. Here n denotes the radial quantum number and $\hbar M$ the angular momentum. The corresponding eigenfunctions of the effective one-particle Hamiltonians are given by

$$\langle \mathbf{r} | nM \rangle = \frac{1}{\sqrt{2\pi\lambda}} \exp(iM\varphi) \phi_{nM} \left(\frac{r^2}{2\lambda^2} \right) \quad (5)$$

in both cases, where the characteristic length λ is defined by $\lambda^2 = \hbar/(2m\omega_{\text{eff}})$. The only difference results from the relevant mass, which is $m = 2m^*$ for the c.m. motion

and $m = m^*/2$ for the relative motion. The radial wave functions are given by

$$\phi_{nM}(\xi) = \sqrt{n!/(n+|M|)!} \exp(-\frac{1}{2}\xi) \xi^{|M|/2} L_n^{(|M|)}(\xi) \quad (6)$$

with $L_n^{(|M|)}$ a Laguerre polynomial. The Coulomb interaction partly lifts the degeneracies of the total energy spectrum, $E_{n_C, M_C; n_R, M_R} = \varepsilon_{n_C M_C} + \varepsilon_{n_R M_R}$, but due to the rotational invariance it does not couple states with different angular momenta M_R of the relative motion. It is easily shown that the degeneracy $E_{n_C, M; n_R, -M} = E_{n_C, -M; n_R, M}$ still holds in the presence of the Coulomb interaction, which, of course, does not affect the c.m. motion.

In view of the square arrays of quantum dots investigated in experiments,⁵ we consider deviations from the parabolic confinement of the form

$$U(\mathbf{r}) = \frac{1}{2} m^* \omega_4^2 (a r^4 + b x^2 y^2), \quad (7)$$

with ω_4 , a , and b constants, i.e., the confining potential has at least square symmetry. Even in the case of circular symmetry ($b = 0$) this additional potential couples the RM and c.m. of quantum-dot helium. As a consequence, the generalized Kohn's theorem is no longer applicable. Accordingly, additional resonances are to be expected in FIR spectra reflecting internal features of the quantum system.

We treated the two-particle problem numerically by diagonalizing the Hamiltonian matrix. In the representation (3), explicit formulas for the matrix elements of the Coulomb potential as well as the confining potential $U(\mathbf{r})$ can be obtained. To achieve an accuracy of about 99% for the low-lying energies and eigenstates, the radial quantum numbers $n_{C,R} = 0, \dots, 15$ and the angular momenta $M_{C,R} = -5, \dots, +3$ were taken into account. Due to the square symmetry even and odd angular momenta do not couple. Therefore the problem divides into four decoupled (sparse) subsystems.

To investigate the FIR response, we first calculated the low-energy eigenvalues and eigenstates and, then, used these results to calculate the dipole matrix elements. Thus, we were able to evaluate the frequency spectrum and the oscillator strength of the FIR excitations. For the strictly parabolic confinement ($\omega_4 = 0$), we reproduced the recent results of Merkt, Huser, and Wagner.⁷ For the following it is important to note that, as a consequence of the Coulomb repulsion, the ground state of the RM occurs with increasing values of the magnetic field at increasingly higher angular momenta (larger values of $-M$). We use the notation $|n_C M_C; n_R M_R\rangle$ for the (product) eigenstates of the interacting two-electron system with parabolic confinement. It turns out that, for small values of n_R , these states have a large overlap ($> 90\%$) with the corresponding eigenstates (3) of the noninteracting system.

Figure 1 shows the result for a circular symmetric confining potential. Only resonances with oscillator strength exceeding 1% are drawn. The sum of these oscillator strengths turns out to be greater than 99.9%. For mag-

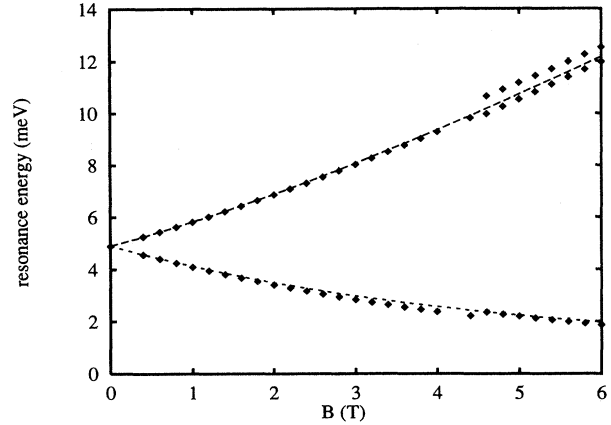


FIG. 1. FIR resonance spectrum of quantum-dot helium with circular symmetric deviations from the parabolic confinement potential. Parameters in Eq. (7): $\hbar\omega_0 = 3.37$ meV, $\omega_4/\omega_0 = 10^{-5}$, $a = 1/\text{\AA}^2$, and $b = 0$. Only resonances with oscillator strengths exceeding 1% are plotted. Dashed lines: fit to Eq. (1).

netic fields $B \leq 4.6$ T the spectrum is similar to that of parabolic dots (with $\omega_0 = 4.89$ meV instead of 3.37 meV), i.e., just the two resonances ω_{\pm} are observable. For $B \geq 4.8$ T the upper mode (ω_+) splits into two resonances. Such a behavior has been observed by Demel *et al.*⁵ in systems with about 210 electrons per dot and very recently by Meurer, Heitmann, and Ploog² on arrays with two electrons per dot.

The blueshift of the spectrum is not unexpected: both transitions occur between states with different angular momenta ($|\Delta M| = 1$). But the higher the angular momentum of a state the larger is its spatial extend, and the more it is affected by the r^4 potential. Moreover, as was pointed out by Gudmundsson and Gerhardt,¹⁴ a transformation of $U(\mathbf{r})$ into c.m. and RM coordinates yields an additional harmonic contribution to the c.m. Hamiltonian which for our parameter values accounts for a blueshift of 1.1 meV.

In our calculations the splitting of the ω_+ mode occurs at the same magnetic field value ($B = 4.8$ T) at which the angular momentum of the ground state switches from $M_R = 0$ to $M_R = -1$. This happens because in the more extended $M = -1$ state the Coulomb repulsion energy is lower than in the $M = 0$ state, which according to Eq. (4) at sufficiently high magnetic field has only a slightly lower kinetic energy. For $B < 4.8$ T the dipole transition belonging to the ω_+ mode takes place between the ground state, which evolves from and is very well approximated by $|00; 00\rangle$, and the state $|01; 00\rangle$, which is nondegenerate. For $B \geq 4.8$ T the ground state has an overlap of more than 99% with the state $|00; 0-1\rangle$. In the parabolic confinement, the ω_+ transition leads to the state $|01; 0-1\rangle$, which is degenerate with $|0-1; 01\rangle$, even with full inclusion of the Coulomb interaction. Both these states become coupled by the nonparabolic r^4 part of the confining potential (note: the total angular momentum of $|01; 0-1\rangle$ and $|0-1; 01\rangle$ is the same, $M = M_R + M_C = 0$). Thus, the eigenstates in the non-parabolic confinement poten-

tial resulting from the coupling of these two states both contain a contribution of the $|01;0-1\rangle$ state. Therefore dipole transitions to both states become allowed, showing up in a splitting of the upper resonance.

For the chosen parameters, the deviations from the parabolicity of the confining potential are small. Consequently, coupling of the states $|01;00\rangle$ and $|01;0-1\rangle$, which can be reached by dipole transitions from the ground state, by the r^4 potential to other states, which are nondegenerate with one of them, leads only to additional dipole-allowed transitions with negligible oscillator strength, which are not observable.

Deviations from the circular symmetry give rise to further resonances. This situation is shown in Fig. 2(a): At a magnetic field $B = 2.4$ T the anticrossing of the ω_+ line with a second line becomes evident. For this magnetic field the states $|01;00\rangle$ and $|0-1;0-2\rangle$ are accidentally degenerate in the parabolic (as well as in the circular symmetric) potential. The x^2y^2 term of the confining potential couples these two states, and thus lifts the degeneracy. This term allows for coupling of states with a total angular momentum difference of 4, i.e., states with angular momenta M_R and M_C become coupled to states which differ from these in both M_R and M_C by ± 2 , or in only one of these quantum numbers by ± 4 . This coupling is strong enough to provide both transitions with considerable oscillator strength within a finite range of magnetic fields, $2.1 \leq B \leq 2.8$ T. This does not hold for the very similar crossing of the $|01;00\rangle$ line and the $|0-3;00\rangle$ line at $B = 3.4$ T, which corresponds to a coupling of states differing only in the c.m. angular momentum. Here the coupling is so weak that a second line only appears in the small range of $3.3 \leq B \leq 3.5$ T. Moreover the line splitting of less than 0.23 meV is hardly resolvable. The occurrence of two anticrossings is caused by the Coulomb interaction of the electrons. Without this interaction the states $|0-1;0-2\rangle$ and $|0-3;00\rangle$ are degenerate. But due to the larger spatial extend of its RM wave function, the Coulomb energy of the first is smaller, leading to the anticrossing at a lower magnetic field.

The difference between both anticrossings is originated in the corresponding potential matrix elements, $\langle 01;00|U(\mathbf{r})|0-1;0-2\rangle$ and $\langle 01;00|U(\mathbf{r})|0-3;00\rangle$, respectively. While the energy splitting at the crossing (of the unperturbed spectra) is proportional to this matrix element, the oscillator strengths are proportional to its square. Since the matrix element belonging to the anticrossing at $B = 2.4$ T is larger than that for $B = 3.4$ T by a factor of $\sqrt{3}$, this accounts for the smaller energy splitting of the second anticrossing as well as the smaller magnetic field range where both lines are observable.

Experimentally the anticrossing behavior of the ω_+ resonance has been observed in the measurements of Demel *et al.*⁵ indicating that the confinement potential in their systems has contributions with only quadratic symmetry. As has been argued by Gudmundsson and Gerhardt¹⁴ the oscillator strengths of the $|01;00\rangle$ - $|0-3;00\rangle$ anticrossing decreases with the number N_e of electrons per dot as $1/N_e$, since the characteristic length of the c.m. motion, cf. Eq. (5), decreases as $N_e^{-1/2}$. Thus it cannot be seen in this experiment, where $N_e = 210$.

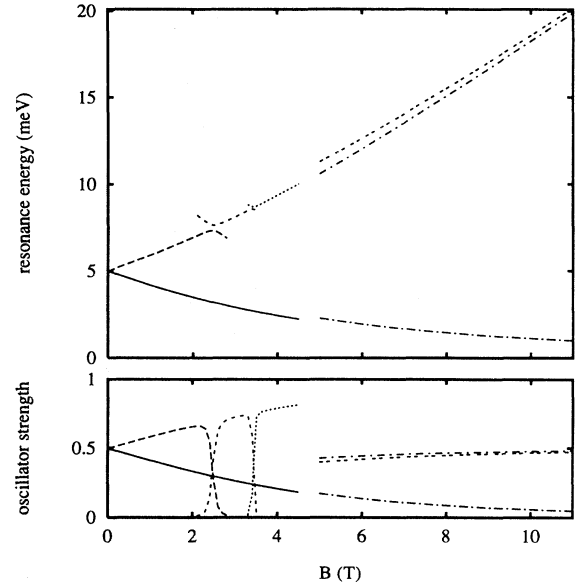


FIG. 2. (a) FIR resonance spectrum for a square symmetric confining potential. Parameters: as Fig. 1, but $b = 1/\text{\AA}^2$. A lifting of the degeneracy of the ω_{\pm} resonances at $B = 0$ T is not resolved for the chosen parameters. (b) Oscillator strengths corresponding to (a). Equal line styles in (a) and (b) refer to the same resonance mode.

The discontinuity in the oscillator strength of the ω_+ mode [Fig. 2(b)] is due to the line splitting. Both resonances for $B \geq 4.8$ T share the strength of the ω_+ resonance for $B < 4.8$ T. The sharp transition, however, is an artifact of our calculation: Taking into account finite temperatures (and a finite linewidth of the resonances) would smear out the discontinuity.

In summary, we showed that even small deviations from the exceptional case of a *strictly* parabolic dot confinement allow for FIR spectra with a rich structure. They are strongly influenced by Coulomb interaction effects, though the main features of the collective excitations, i.e., a rigid c.m. motion (ω_{\pm} mode), remain dominant. In particular, the occurrence of the second ω_+ mode is due to the fact that the ground state changes with increasing magnetic field from a state with RM angular momentum $M_R = 0$ to a state with $M_R = -1$. This is a consequence of the Coulomb interaction and enables dipole transitions to a pair of states, which are degenerate in parabolically confined quantum dots and become mixed by the nonparabolic perturbing potential. The anticrossing behavior, on the other hand, appears also in a noninteracting system. However, the Coulomb interaction lifts the degeneracy of the states which may lead to such crossings and shifts the magnetic field, at which the dominant anticrossing occurs, to lower values. Although the results presented here are obtained for a two-particle system, they reveal the essential mechanisms leading to the resonance structures observed also in experiments on quantum dots with a larger number of electrons.

We acknowledge stimulating discussions with D. Heitmann, B. Meurer, and V. Gudmundsson.

- ¹J. Alsmeier, E. Batke, and J.P. Kotthaus, *Phys. Rev. B* **41**, 1699 (1990).
- ²B. Meurer, D. Heitmann, and K. Ploog (unpublished).
- ³A. Lorke, J.P. Kotthaus, and K. Ploog, *Phys. Rev. Lett.* **64**, 2559 (1990).
- ⁴Ch. Sikorski and U. Merkt, *Phys. Rev. Lett.* **62**, 2164 (1989).
- ⁵T. Demel, D. Heitmann, P. Grambow, and K. Ploog, *Phys. Rev. Lett.* **64**, 788 (1990).
- ⁶P.A. Maksym and T. Chakraborty, *Phys. Rev. Lett.* **65**, 108 (1990).
- ⁷U. Merkt, J. Huser, and M. Wagner, *Phys. Rev. B* **43**, 7320 (1991).
- ⁸P. Bakshi, D.A. Broido, and K. Kempa, *Phys. Rev. B* **42**, 7416 (1990).
- ⁹Q.P. Li, K. Karraï, S.K. Yip, S. DasSarma, and H.D. Drew, *Phys. Rev. B* **43**, 5151 (1991).
- ¹⁰W. Kohn, *Phys. Rev.* **123**, 1242 (1961).
- ¹¹V. Shikin, S. Nazin, D. Heitmann, and T. Demel, *Phys. Rev. B* **43**, 11 903 (1991).
- ¹²S.J. Allen, Jr., H.L. Stormer, and J.C.M. Hwang, *Phys. Rev. B* **28**, 4875 (1983).
- ¹³D.A. Broido, K. Kempa, and P. Bakshi, *Phys. Rev. B* **42**, 11 400 (1990).
- ¹⁴V. Gudmundsson and R.R. Gerhardts, *Phys. Rev. B* **43**, 12 098 (1991).
- ¹⁵T. Chakraborty, V. Halonen, and P. Pietiläinen, *Phys. Rev. B* **43**, 14 289 (1991).